

Inelasticity and intranuclear cascading in geometrical multichain model

T. Wibig

Experimental Physics Dept., University of Lodz, Pomorska 149/153, 90-236 Lodz, Poland

(October 16, 2018)

The inelasticity in nucleus-nucleus collisions at high energies is calculated in the framework of geometrical multichain model. The very fast increase of the inelasticity is found as a result of a second-stage cascading process. The same behaviour is expected for all the models using the wounded nucleon idea. The simple formula for the number of wounded nucleons inside colliding nuclei does not need to be exact.

I. INTRODUCTION

The inelasticity in nuclei collisions is one of the most important properties of the interaction from the point of view of hadronic cascade development in matter. Cosmic-ray extensive air shower (EAS) physics is a particular domain where the knowledge of inelasticity is extremely important.

The definition of inelasticity itself is a problem. The definition which is a subject of this paper will be given in the next section in a useful form for EAS development studies (in the laboratory system of reference). Generally the inelasticity can be understood as a fraction of interaction energy transferred to secondary particles created in the interaction. The remaining energy is carried by the “leading particle” and transported downward to next rank interaction in the hadronic cascade. Thus, the inelasticity is determined by the mechanism of multiparticle production. In this paper quantitative results obtained from particular model calculations will be given.

Initially the geometrical two-chain model (G2C) was developed to describe relatively low-energy hadron-hadron interactions [1]. Recently [2] the geometrical multichain (GMC) extension of the model to very high energies was presented. Obtained proton-proton multiparticle production characteristics show that up to at least SPS energies the underlying physics can be treated as competitive with that used by dual parton-like models or relativistic jet (LUND-like) idea. The straightforward way of the extension of the G2C (and, of course, GMC) model to proton-nucleus and more: to nucleus-nucleus interactions was discussed in [3,4]. The possibility of introducing geometrical chains in the framework of wounded nucleon picture was used to obtain some results on inelasticity for proton-nucleus collisions. Comparison with the available data encourage further examinations.

In this paper we would like to present GMC model extension to nucleus-nucleus interactions. The special attention will be paid to chain formations in the intranuclear cascading process.

The very old and naive picture (simple superposition) was the first attempt to the problem but it was disqualified on a very early stage by experiments (see, e.g. [5]). Then the idea of wounded nucleons arose and it was generally accepted. It can be expressed in the statement that once one of projectile nucleons interacts inelastically with the one from a target nucleus intermediate states called “wounded nucleons” are created. The spatial extension of the wounded nucleon is the same as original nucleon before the collision. The subsequent collisions inside the target nucleus take place before this “excited state” hadronize. The non-zero time interval between excitation and hadronization is confirmed by for example, Bose-Einstein correlation study. Its value depends on particular definition (it is frame dependent) but it is generally accepted to be of order of at least 1 fm.

In the wounded nucleon idea for proton-nucleus collisions each subsequent interaction of the once wounded nucleon leads to the excitation of one of nucleons from the target. So, in a first approximation, it adds to the overall average multiplicity about $\frac{1}{2}$ of p - p multiplicity (for respective interaction energy) and leads to the rather small decrease of the incoming wounded nucleon energy (due to momentum and energy transfer). This general picture is confirmed very well in many experiments.

Similar results are obtained in DPM-like proton-nucleus pictures where the first interaction inside the target creates two quark-gluon strings stretched generally between valence quarks of two colliding hadrons. The next interactions each produce each two additional strings but their quark ends are formed by the sea quarks on the projectile side thus leading to $\sim 1/2$ of p - p multiplicity addition and also to the small change of the main projectile string energy and momentum.

The situation becomes more complicated when nucleons are involved on both, target and projectile, sides. In this case there can also appear, among others, collisions of two wounded nucleons. The introduction of wounded nucleons on both colliding nuclei leads to the further decrease of the mean multiplicity (and inelasticity) per one intranuclear interaction. Anyhow, this can be solved quite natural by careful investigation of the so-called intranuclear cascade.

In both, DPM- and LUND-like interaction models the creation of all chains (strings) can be performed and is well known (e.g. in FRITIOF realization of the LUND picture [6] and DTUJETII for DPM [7]) for some time.

The next step in all models existing so far is to perform the hadronization of wounded nucleons (chains, strings, excited states). The hadronization as a typical soft process has to be treated by phenomenological models which use more or less theoretically justified assumptions. The GMC model also treats the hadronization in a specific way. Differences were discussed in [1,2]. Despite these differences, results given by different models are quite similar. Free parameters of all the models were adjusted to about the same experimental data sample. Anyhow, we do not expect that the details of the hadronization process descriptions can effect the general subject of this paper very much, as will be shown later.

After the hadronization process, the created hadrons could, in principle, appear within one of the colliding nuclei [7]. Thus, there is a possibility that they (if their energies are high enough) can further interact inside the same nucleus. This depends on the freeze-out time — more exactly on the distance traversed by the wounded nucleon in the nucleus rest frame before it hadronizes. Thus, it is expected that when the interaction energy increases this effect vanishes due to Lorentz dilatation (even if the freeze-out time in the wounded nucleon rest system is as small as $1 \div 0.5$ fm, the energy of about 1 TeV/nucleon in laboratory frame, is enough to prevent it from the hadronizing most of the wounded nucleons within the nucleus).

This is the state of art of the majority of contemporary high-energy hadronic interaction models. In this paper we will introduce another sort of intranuclear cascade process.

The creation of wounded nucleons during the passage of one interacting nucleus through the other is in general rather well established [8]. The cascading of newly created hadrons inside both nuclei is quite natural. (The importance of this process decreases with increasing interaction energy due to the finite freeze-out time.) Interactions between excited states (wounded nucleons, chains, strings) is not so straightforward, but has been extensively discussed (see e.g. [9]) as an important contamination in quark–gluon plasma searches and interpretations high transverse energy events. However, the overall effect on minimum bias event studies is not very significant [8]. For the inelasticity studies the influence is expected to be even less due to the fact that the energy of both incoming, earlier excited states has to be conserved in the outgoing wounded states.

However, there is another possibility which we will call hereafter second step cascading: an interaction of wounded nucleon from a (target or projectile) nucleus with another nucleon from the same nucleus before the hadronization occurs. Wounded nucleons excited to relatively high invariant mass in its nucleus rest frame of reference move fast due to the momentum and energy conservation. The effect should intensify with the increasing interaction energy. The first reason for this is the increase of the wounded nucleon energy in the nucleus rest frame. If the energy is high enough the rise of the nucleon–nucleon cross section starts to play an important role in the increase of the probability of subsequent interaction. This probability also increases due to the increase of the range of the wounded nucleon within the nucleus (Lorentz dilatation of the freeze-out time). If this time (or the Lorentz γ factor) is high enough almost all wounded nucleons will abandon the nucleus before secondary hadron creation starts. Of course there could always be cases when wounded nucleon hadronize inside nucleus, for example single-diffraction-type excitations to any small invariant masses.

The great influence of second step cascading process is straightforward. On the projectile side (high laboratory energy) the excitation of one initially untouched nucleons by an excited state going backward in antilaboratory frame of reference leads to a transfer of a part of nucleon energy to the secondary produced particles. Their energy in the nucleus center-of-mass system (CMS) are rather small but after transformation to the laboratory system the effect is expected to be quite considerable.

II. THE GMC MODEL

The GMC model differs from the other known interaction models (DPM or LUND-type relativistic string model) in details of the treatment of the creation of “wounded nucleons” (excited states, chains, strings). The idea of using structure functions to extract the interacting valence quark from colliding hadrons and control colour and/or momentum flow has some advantages, of course mainly in the reduction of number of free parameters in a model. It moves the problem of structure function determination (thus, momenta of quarks) from adjusting them by comparing model expectations to data with the other kind of physical experiments outside the soft hadronic scattering domain. This made the high-energy interaction modelling more reliable and suited it in a wide context of the high energy-physics, or physics in general. In the GMC model a phenomenological description of the chain creation is used with very few parameters to be adjusted directly to the soft hadronic interaction data. On one hand, this can be treated as

a limitation of the model but, on the other hand, it can, of course, give a better data description. Some connections between the GMC model and structure function approach exist, and both ways are, in some sense, equivalent.

The geometrization of the interaction picture is in the parametrization of the multiparticle production process as a function of the impact parameter of colliding hadrons. As was shown, for example in [1], the elastic scattering data can lead to quite an accurate determination of a “matter” distribution inside hadrons. To avoid the energy dependence of the hadronic cross section the hadron sizes are assumed to be scaled [10] according to an energy-dependent factor r_0 defined by:

$$\sigma_{\text{inel}} = \pi r_0^2. \quad (1)$$

The hadron opacity function Ω is associated with the hadron matter density distribution ρ and can be determined precisely from the elastic scattering data at relatively low energies. If one denotes by E_0 the energy for which this determination was performed then the geometrical scaling can be expressed in the following way

$$\Omega(b) = \int d^2r \rho_1(\tilde{b}) \rho_2(\tilde{b} - r) \quad (2)$$

where \tilde{b} is the scaled impact parameter defined as:

$$\tilde{b} = b \sqrt{\frac{\sigma_{\text{inel.}}(E_0)}{\sigma_{\text{inel.}}(E)}}. \quad (3)$$

The geometrical scaling gives a number of predictions concerning energetic behaviour of, for example cross section ratios, multiplicity distributions or differential elastic cross sections. Some of them are confirmed experimentally quite strongly such as KNO scaling (for soft components) whilst others are questioned such as $\sigma_{\text{elastic}}/\sigma_{\text{total}}$. However, slight modifications of general idea presented above can restore the agreement with the observations. A very good example is given in [11]. It is shown that slow increase of hadronic central opacity can be responsible for the observed change of elastic-to-total cross section ratio and elastic scattering slope change from ISR to SPS energies. However, this does not interfere with our geometrical approach. As will be shown below, the main properties of hadronization depend on the ratio of the opacities at given b to the central one. The change in cross section values for nucleus–nucleus collision is negligible.

For the multiparticle production processes it can be expected that more peripheral collisions should lead to less excited intermediate states. The parametrization which describes quite well many characteristics seen in experiments was found [1] to be:

$$M_{\text{chain}} \sim M_0 + \left(\frac{\Omega(b)}{\Omega(0)} \right)^\alpha \left(\frac{\sqrt{s}}{2} - M_0 \right) \quad (4)$$

where M_{chain} is a chain invariant mass, \sqrt{s} is interaction CMS available energy, M_0 is a mass of the lightest hadron which can be formed from the particular quark contents, and Ω is defined in the Eq.(2). α is one of the model parameters found to be equal to 0.48.

After the chain mass creation each chain moves independently according to energy-momentum conservation law for the time equal to “freeze-out” time assumed to be a constant and energy independent in a chain rest system. Later the hadronization occurs. Due to the subject of this paper details are not very important. They can be found in [2] where some results are given for $\sqrt{s} \sim 20$ GeV and SPS energies. In general, the particles are created uniformly in the phase space with limited transverse momenta taken from the exponential distribution in m_\perp^2 . Flavours and spin states are generated according to commonly accepted rules (with some slight modifications). For the very high energies (chain masses) the gluon brehmsstrahlung process can take place leading to the prehadronization break-ups of the initial chain.

III. INELASTICITY

The general subject of this paper is the inelasticity behaviour of nucleus–nucleus interactions. The inelasticity can be defined in many ways. The definition used here is:

$$\begin{aligned}
K_{\mathcal{NN}} &= \frac{\langle \text{Energy carried by produced secondaries} \rangle}{\text{Initial energy of the projectile nucleus}} = \frac{E_{\text{sec}}^f + E_{\text{sec}}^b}{E_{\text{in}}} = \\
&= \frac{(E_{\text{w.n.}}^f - E_{\text{lead.}}^f) + E_{\text{w.n.}}^b}{E_{\text{in}}} = \frac{E_{\text{w.n.}}^f k_{\text{pp}} + E_{\text{w.n.}}^b}{E_{\text{in}}} = \xi^f k_{\text{pp}} + \xi^b
\end{aligned} \tag{5}$$

where superscripts f and b denote projectile (forward) and target (backward) chains, $E_{\text{w.n.}}$ is an average energy of wounded nucleons and $E_{\text{lead.}}$ is the mean energy of leading barions created in the final hadronization of created chains. All energies are given in laboratory system of reference. The factor $(1 - k_{\text{pp}})$ denotes an average fraction of wounded nucleon (chain) energy carried by the leading barion created from this particular chain. It is defined as:

$$1 - k_{\text{pp}} = \frac{1}{E_{\text{w.n.}}^f} \left(E_{\text{proton}}^f + E_{\text{neutron}}^f - E_{\text{anti-proton}}^f - E_{\text{anti-neutron}}^f \right). \tag{6}$$

Values of k_{pp} obtained in the framework of the GMC model for different interaction energies are given in Table I.

TABLE I. The inelasticity in proton-proton interactions in the GMC model for different energies.

E_{lab} [GeV]	\sqrt{s} [GeV]	k_{pp}	K_{pp}
10	4.5	0.20	0.29
10^2	13.8	0.32	0.43
10^3	43.4	0.34	0.45
10^4	137.	0.36	0.46
10^5	433.	0.38	0.47
10^6	$1.4 \cdot 10^3$	0.39	0.48
10^7	$4.3 \cdot 10^3$	0.40	0.49
10^8	$1.4 \cdot 10^4$	0.40	0.49
10^9	$4.3 \cdot 10^4$	0.40	0.49

It should be remembered that values of k_{pp} (third column in Table I) are of course different than the common proton–proton inelasticity defined as $K_{pp} = [E_{lab} - (E_{proton} + E_{neutron} - E_{anti-proton} - E_{anti-neutron})] / E_{lab}$ (values are given for a comparison in the fourth column in the Table I).

As one can see in the GMC model, the inelasticity of proton–proton K_{pp} as well as the “chain inelasticity” k_{pp} is almost constant for energies of interest — higher than ~ 100 GeV ($\sqrt{s} \sim 15$ GeV). This result confirms the suggestion presented in [12] that a rise of the average p_{\perp} and mean multiplicity with energy does not necessary lead to an increase in the proportion of energy needed to create the secondary particles. The constancy of inelasticity is not in contrast to available accelerator data.

The average energy losses in a constant amount of matter traversed are responsible for a development of nuclear cascade in media. For a description of a particle passage through the matter, the behaviour of the inelastic cross section is as important as the inelasticity in each individual interaction. The rise of the proton–proton cross section seen in the high-energy range is well known and measured precisely up to about 10^{15} eV of proton energy in the laboratory system of reference. It is obvious that this should manifest itself in the proton–nucleus and nucleus–nucleus cross section behaviour as well.

In the geometrical scaling picture the inelastic proton–proton cross section is given by:

$$\sigma_{pp}^{inel}(b) = 1 - \exp(-2\Omega(b)) \quad (7)$$

where Ω is defined in Eq.(2) and is scaled due to the cross section increase with energy. The extension to the nucleus–nucleus interaction according to the Glauber approach leads to the formula:

$$\sigma_{NN}(b) = 1 - \int \prod_{n=1}^A d^2b_{An} T(b_{An}) \prod_{m=1}^B d^2b_{Bm} T(b_{Bm}) [1 - d\sigma_{pp}(b - b_{An} + b_{Bm})] \quad (8)$$

where $T(b)$ is a nucleus profile function, b - an impact parameter of nucleus-nucleus collision and b_{An} is a position of the n th nucleon of the nucleus A on the impact parameter plane.

Further simplifications of Eq.(8) are often used to calculate nucleus–nucleus cross section. The main is an optical approximation which treats σ_{pp} in Eq.(8) as equal to the δ function multiplied by respective value of proton–proton cross section. Sometimes also an overall opacity of the nucleus as a whole is calculated by integration of nucleon–nucleon opacity with the nucleus profile function. Such a treatment leads directly to a result similar to the one given in Eq.(7) with the respective nucleus opacity instead of Ω defined originally for hadronic collision. As will be shown below, differences between results obtained with and without such approximations increase with energy reaching about 30% at highest energies seen in cosmic rays. However, it has to be remembered that the extrapolation of the proton–proton cross-sections so much further from the region of direct measurements is much more uncertain. In this paper the exact numerical integration of Eq.(8) was used as a method for nucleus–nucleus cross section calculations.

The nucleus profile function is obtained as a projection of the nucleus density. The assumed density is

$$\varrho(R) = \begin{cases} \frac{A}{(a\sqrt{\pi})^3} \exp\left[-\left(\frac{R}{a}\right)^2\right] & \text{for } A < 40 \\ \frac{\rho_0}{1 + \exp[(R-c)4.4/t]} & \text{for } A \geq 40 \end{cases} \quad (9)$$

which is Gaussian and of Fermi type for lighter and heavier nuclei, respectively.

The parameters of that formula are fitted to describe the data on the inelastic cross section. Details are given in [4].

In most of cross section calculations a lack of any correlation between nucleons inside the nucleus is assumed. Of course it is quite obvious that two nucleons can not be very close to each other. In the present calculations the minimal distance between each pair of nucleons inside the nucleus was set equal to 0.8 fm.

Fig. 1 presents energy dependencies of nucleus–nucleus cross sections for iron-nitrogen collisions (these nuclei are chosen because of their importance in the cosmic ray (EAS) physics) and p – p cross sections obtained from the Regge theory-inspired formula [13]:

$$\sigma_{pp} = 56 (\sqrt{s})^{-1.12} + 18.16 (\sqrt{s})^{0.16} \quad (10)$$

fitted to the available accelerator data.

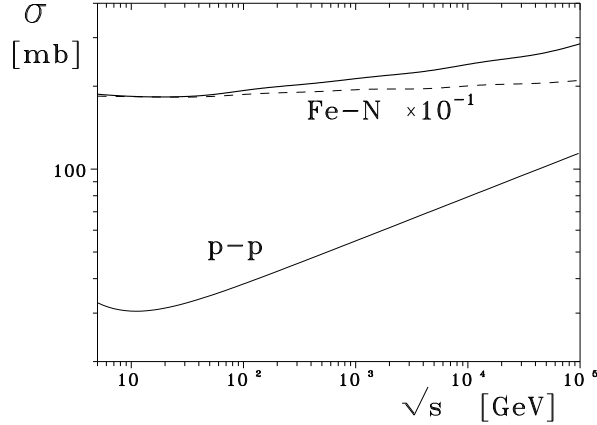


FIG. 1. Cross section for p - p interaction used in the present calculations and the calculated Fe-N inelastic cross section. The broken curve represents the result obtained using the optical approximation and the full curve represents the geometrical scaling.

The number of nucleons participating in the inelastic nuclei collision is related closely to the respective cross section ratios and studied extensively in nucleus-nucleus interaction examinations. The commonly used approximation based on the optical approach gives:

$$n_A = \frac{A\sigma_{pB}}{\sigma_{AB}} \quad n_B = \frac{B\sigma_{pA}}{\sigma_{AB}} \quad \nu_{AB} = \frac{AB\sigma_{pp}}{\sigma_{AB}} \quad (11)$$

where n_A is the average number of participants from A nucleus and ν_{AB} is the average number of intranuclear inelastic nucleon-nucleon collisions in the A - B interaction. In the Fig. 2 the distributions of number of nucleons participating in Fe-N collisions for different interaction energies are given. Broken curves represent the approximation used in evaluation of Eq.(11). This approach, however, does not take into account the second step cascading mechanism described qualitatively above. Thus, these lines depict only the “primarily wounded” nucleons in each colliding nucleus. This means that they interact inelastically during the passage of one nucleus through the other (the first step cascading). After this the second step cascading takes place. The primarily wounded nucleons inside each nucleus moves back and, when they traverse its own nucleus, they can excite nucleons which survives the “primary” collision (with nucleons from the other nucleus). Cross sections for the second step cascading interaction are the same as for p - p collision at respective CMS energy. Thus no additional parameters are needed to describe the second step cascading process. The effect presented in Figs. 1 and 2 is independent on a particular Monte Carlo realization. Small differences in p - p cross sections are negligible here.

The second step cascading process has to increase of the number of excited nucleons in both colliding nuclei. Results of our complete collision calculations are given in the Fig. 2 by the full histograms.

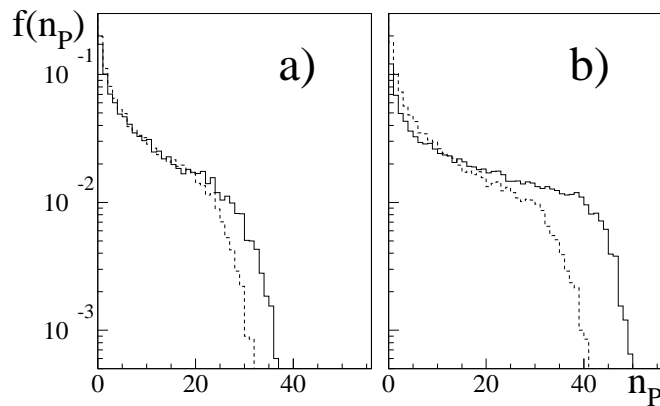


FIG. 2. Distributions of the number of wounded nucleons in projectile (iron) nucleus in the Fe–N collision for interaction energies, E_{lab} is equal to (a) 100 GeV and (b) 10^6 GeV. The broken and full curves represent results without and with second step cascading, respectively.

The importance of second step cascading for the number of wounded nucleons is seen even better in the Fig. 3 where the mean values of the wounded nucleon numbers are given as a function of interaction energy. The effect is stronger on the projectile (heavier) nucleus side.

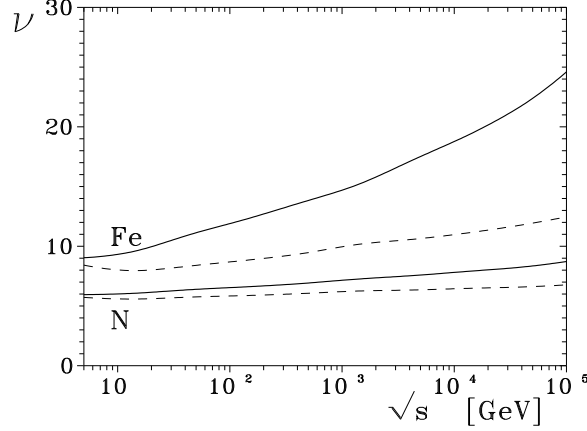


FIG. 3. Average wounded nucleon number for Fe–N interaction. The two upper curves are for iron, the lower curve for nitrogen nucleus respectively. Broken curves show the number of primary wounded nucleons (before second step cascading), full curves represent final wounded nucleon numbers (after second step cascading process).

The increase of the number of wounded nucleons has to lead to an increase of the inelasticity no matter how it is defined. To give the quantitative description of this increase we will use the definition in Eq.(5). For this the average energy carried by wounded nucleons is needed. It is obtained from the detailed GMC model Monte Carlo calculations of nucleus–nucleus collisions tracking each nucleon in both nuclei during its passage through the other and after this an eventual traverse through its own nucleus up to the hadronization phase began. The respective distributions are presented in Fig. 4 for two different energies and the respective average values as a function of interaction energy are shown in the Fig. 5. Broken curves show the results without second step cascading, full curves represent our final results. Dotted histograms gives the energy fractions carried by CMS backward-going chains — “wounded nucleons” from the target.

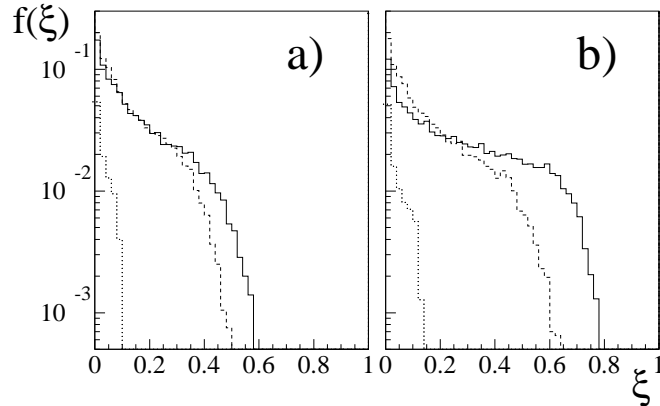


FIG. 4. Distributions of the energy fraction carried by wounded nucleons (per 1 nucleon) in the Fe–N collision for interaction energies, E_{lab} is equal to (a) 100 GeV and (b) 10^6 GeV. The broken and full curves represent results without and with second step cascading, respectively. Dotted histograms shows the energy fractions carried by wounded nucleons from the target (divided by 10).

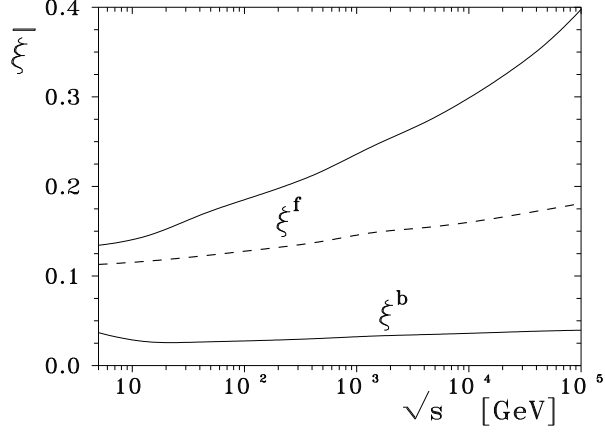


FIG. 5. Fraction of the laboratory energy carried by wounded nucleons after the Fe-N collision. The broken and full curves represent results of calculations without and with second step cascading, respectively.

These results together with the chain inelasticities (k_{pp}) listed in Table I can be used to calculate the average inelasticity in Fe-N collisions (Eq.(5)). The final result is presented in Fig. 6.

As can be seen, the introduction of the second step cascading process leads to a significant increase of inelasticity in nucleus-nucleus collisions. The excess over the standard cascading calculation results achieve a factor of 2 at the energies of the order of the highest seen in cosmic rays (about 10^{20} eV).

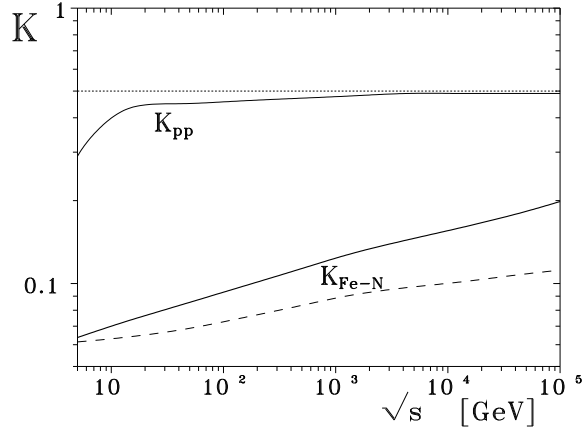


FIG. 6. Inelasticity coefficient of proton-proton and Fe-N collision for different interaction energies. Broken and full curves labeled by K_{Fe-N} were obtained without and with second step cascading process taken into account, respectively.

The review of some interaction properties of different interaction models (VENUS, QGSM, SIBYLL, HDPM, and DPMJET) is presented in [14]. It contains, among others, also values of inelasticity for proton-proton and Fe-N collisions around interaction laboratory energy 10^{15} eV. It is important to note that all the models tested there are introduced to the CORSIKA [15] Monte Carlo program for EAS simulations, so they also are adjusted to cosmic-ray data, while GMC model parameters are obtained using only accelerator data. Most of models listed above give $p-p$ inelasticities much higher (0.67, 0.67, 0.64, 0.53, and 0.74, respectively) than the one obtained from the GMC model (0.49) at 10^{15} eV. In view of the nucleus-nucleus interactions, two models (QGSM and SIBYLL) give the inelasticity close to the one obtained from GMC model without second step cascading process (0.093, 0.097 in comparison with .091). Three other (VENUS, HDPM, and DPMJET) give values close to the one of GMC with second step cascading (0.14, 0.12, and 0.14 in comparison with 0.13). HDPM is the extrapolation of the phenomenological parametrization of low-energy data (DPM inspired). The other models are strongly based on the DPM interaction picture. From the above comparison it is hard to form any conclusive statements. Difficulties with the reproduction of some interaction characteristics measured in accelerator experiments by different models presented also in [14] additionally confirm such conclusion.

IV. SUMMARY

From the point of view of the geometrical multichain model it is quite obvious that the intermediate process should take place in between initial wounded nucleons production and the hadronization. The importance of this new process is that it effects the number of wounded nucleons (chains in GMC) leading to an increase of the inelasticity in nucleus–nucleus interactions. The second step cascading in nucleus-nucleus collisions leads to the significant increase on the inelasticity and wounded nucleon numbers.

This is responsible for much faster dissipation of the nucleus energy while traversing through matter. Change, in comparison with the conventional wisdom, of the overall picture of the hadronic cascades initiated by nuclei is expected toward a faster development on the first stage before the nucleus fragment completely. This can be observed in EAS experiments where position of shower maxima is higher than expectations based on many different Monte Carlo simulation calculations (see, e.g. [16]). The change of inelasticity with interaction energy introduced by second step cascading can also influence the rise of the EAS maximum position with primary cosmic-ray particle energy (see, e.g. [17]) which is also one of the important problems in EAS data interpretation.

-
- [1] T. Wibig and D. Sobczyńska, Phys. Rev. **D49**, 2268 (1994); D. Sobczyńska and T. Wibig, Izv. Acad. Nauk Ser. Fiz. **58**, 26 (1994); T. Wibig and D. Sobczyńska, Izv. Acad. Nauk Ser. Fiz. **58**, 29 (1994); T. Wibig and D. Sobczyńska, Phys. Rev. **D50**, 5657 (1994).
 - [2] T. Wibig, Phys. Rev. D **56**, 4350 (1997).
 - [3] T. Wibig and D. Sobczyńska, J. Phys. **G21**, 29 (1995); Czech J. Phys. **45**, 682 (1995).
 - [4] T. Wibig and D. Sobczyńska, Phys. Rev. D **48**, 3110 (1993).
 - [5] A. Klar and J. Hüfner, Phys. Rev. D **31** 491 (1985).
 - [6] B. Anderson, G. Gustafson and H. Pi, Z. Phys. C **50**, 405 (1991).
 - [7] G. Battistoni, C. Forti and J. Ranft, Astropart. Phys. **3**, 157 (1995).
 - [8] A. Capella, C. Pajaras and A. V. Ramallo, Nucl. Phys. B **241**, 75 (1984).
 - [9] A. Capella, J. Kwiecinski and J. Tran Thanh Van, Phys. Lett. B **108**, 347 (1982); A. Kaidalov, Nucl. Phys. **A525**, 39c (1991). G. Gustafson, “New Results in the Fritiof Model and collective effects in nuclear collisions”, Lund University Report No. LUTP 92-26 1992 (unpublished).
 - [10] A. W. Chao and C. N. Yang, Nucl. Phys. D **8**, 2063 (1973); J. Dias de Deus, Nucl. Phys. B **59**, 231 (1973); A. J. Buras and J. Dias de Deus, Nucl. Phys. B **71**, 481 (1974).
 - [11] T. T. Chou and C. N. Yang, Phys. Rev. D **32**, 1692 (1985).
 - [12] J. Dias de Deus and A. B. Pádua, Phys. Lett. **B315**, 188 (1993).
 - [13] R. Costaldi and G. Sanguinetti, Ann. Rev. Part. Sci. **35**, 351 (1985).
 - [14] J. Knapp, D. Heck and G. Schatz, *Comparison of Hadronic Interaction Models Used in Air Shower Simulations and of Their Influence on Shower Development and Observables*, Forschungszentrum Karlsruhe Report No. FZKA 5828, Forschungszentrum Karlsruhe, Karlsruhe, Germany, 1996.
 - [15] J. N. Capdevielle *et al.*, *The Karlsruhe Extensive Air Shower Simulation Code CORSIKA*, Kernforschungszentrum Karlsruhe Report No. KfK 4998, Forschungszentrum Karlsruhe, Karlsruhe, Germany, 1992.
 - [16] G. L. Cassiday *et al.*, Astroph. J. **356**, 669 (1990); D. J. Bird *et al.*, Phys. Rev. Lett. **71**, 3401 (1993).
 - [17] T. K. Gaisser *et al.*, Phys. Rev. D **47**, 1919 (1993).